Computational Structural Engineering
An International Journal
Vol. 1, No. 1, pp. 11~20 (2001)

Computational Structural Engineering Institute

Conceptual Design and Wind Load Analysis of Tall Building

S.L. Lee† and S. Swaddiwudhipong

Department of Civil Engineering National University of Singapore Singapore 117576

Received January 2001; Accepted April 2001

ABSTRACT

The paper describes the conceptual design, structural modelling and wind load analysis of tall buildings. The lateral stiffness of the building can be obtained economically through the interaction of core walls with peripheral frame tube and/or bundle of frame tubes and integrated design of the basement. The main structural components should be properly distributed such that the building will deflect mainly in the direction of the applied force without inducing significant response in other directions and twist. The cost effectiveness can be further enhanced through close consultation between architects and engineers at an early stage of conceptual design. Simplified structural modelling of the building and its response in three principal directions due to wind load are included. Effects of the two main structural components on the performances of a 70-story reinforced concrete building in terms of peak drift and maximum acceleration under wind load are discussed.

Keywords: wind load, tall building, peak drift, maximum acceleration

1. Introduction

The rapid development of infrastructure in the past few decades results in a large number of taller buildings being constructed in major cities in the region. The lateral response of such structures have become critical and measures have to be taken to ensure a robust and safe structure satisfying stipulated serviceability requirements. These can be achieved economically through well-conceived structural systems in which structural members are designed to serve several functions and integrated to resist lateral loads effectively. Participation of structural engineers interacting with architects at an early stage in conceptual design enhances further the cost effectiveness of the structural system. The interaction of core walls with periphery frame tube and/or bundle of frame tubes and integrated design of the basement contribute significantly to lateral rigidities of the building. The latter, besides providing the needed resistance to lateral loads through direct bearing action, also renders additional premium spaces for shops, supermarkets and car park. The up-down basement construction, if adopted, permits the construction of the superstructure and substructure to overlap resulting in about 10-20% reduction of the construction time (Lee *et al.*, 1992 and 1996). This paper describes the conceptual design, modelling and wind load analysis of tall buildings including a brief description of a 70-storey reinforced concrete building.

† Corresponding author
Tel.: 874-2150; Fax: 779-1635
E-mail address: cveleesl@nus.edu.sg
: cvesomsa@nus.edu.sg

2. Conceptual Design of Structural System

The ratio of building height above any section to its least cross sectional dimension is usually kept below 6 depending on the intensity and severity of wind and earthquake loads. Lower ratio applies to buildings located in severe earthquake zone and/or frequent strong wind incidences. The design of tall buildings excepting the frame tube members and the shear walls, in mild wind environment and/or low seismic zone is usually proportioned initially based on gravity load requirements and checked against appropriate lateral loads using established computer package. Either allowable stresses in structural members are increased or the load factor reduced as specified by building code if both vertical and lateral loads are con-

sidered together. In the latter case, additional reinforcement and/or increase in member sizes may be required.

In many tall buildings especially where the plan and configuration are irregular, the core wall is placed eccentrically due to architectural requirements. An example is the 70-storey reinforced concrete building constructed in Bangkok. The perspective and typical floor plans of the building are shown in Figs. 1-6. In this building, the core wall housing the lift and staircases are located eccentrically to the left of the building. To alleviate the adverse effect of this eccentricity and to improve the torsional rigidity, two shear walls of 1.5 m thick and a shear wall of 1.0 m thick are introduced from grid points A-1 to A-5, R-1 to Q-5 and A-19 to F-21 respectively as shown in Fig. 2. The 1 m thick shear wall is terminated at the first floor level at the main entrance but the two 1.5 m walls are present up to the 13th floor. A line of braced frames (Fig. 7) is provided along grid line 19 between grid lines C and G from the basement B6 to 1st floor and 5th to 13th floors as shown in Figs. 2 and 4 respectively. This is supplemented by three other braced frames at grid lines 11, 13 and 15 between grid lines A and C from 1st to 5th floors (Fig. 3) to provide the continuity of the transfer of lateral load at these levels. Finally, two smaller frame tubes are placed on the two adjacent sides of the main tube as indicated in Fig. 5, to cater for the eccentricity in the upper portion of the building. One of these smaller frame tubes gradually disappears above the 46th floor (Fig. 6). In this building the periphery frame tube consists of deep spandrel beams and flat columns (Fig. 8). In building where there is no balcony, the periphery spandrel beam can be

Fig. 1. Perspective view of 70-storey reinforced concrete building.

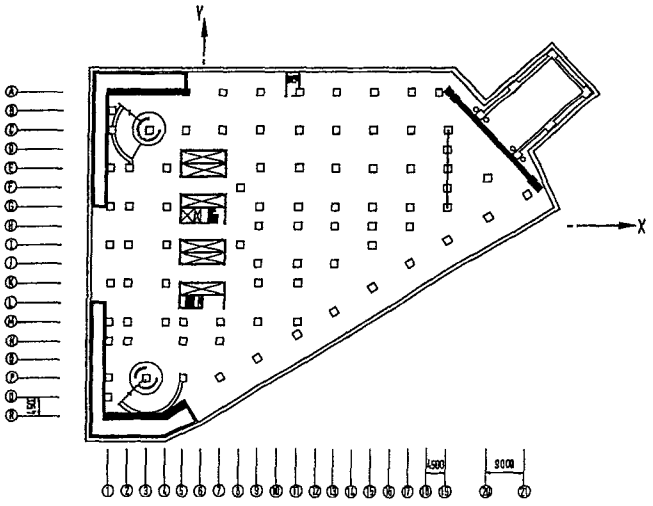

Fig. 2. Typical floor plan for basements.

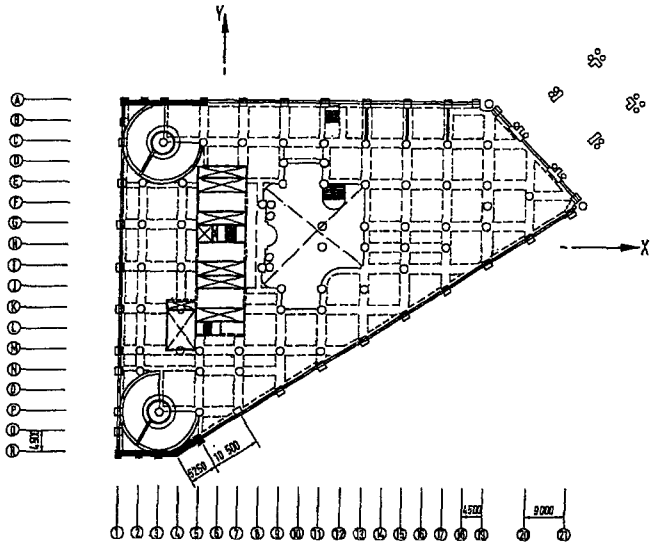

Fig. 3. Typical floor plan, 1st to 5th floors.

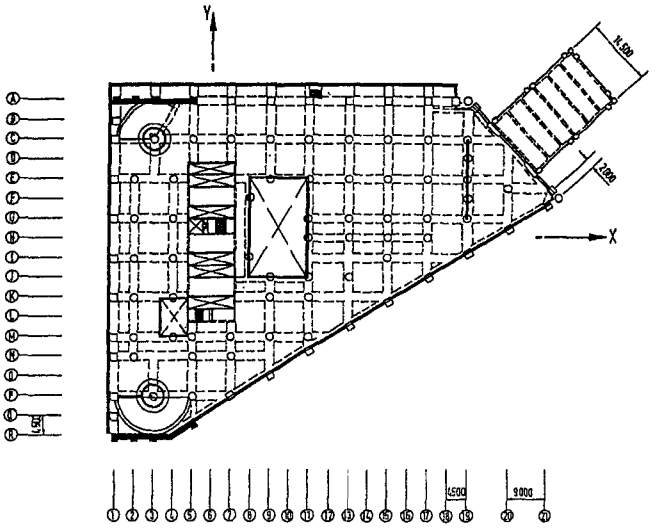

Fig. 4. Typical floor plan, 5th to 13th floors.

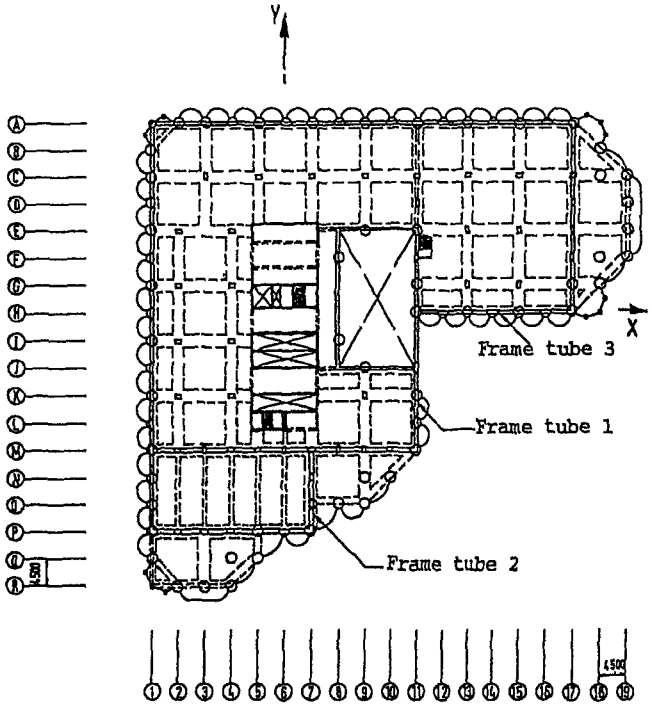

Fig. 5. Typical floor plan, 13th to 45th floors.

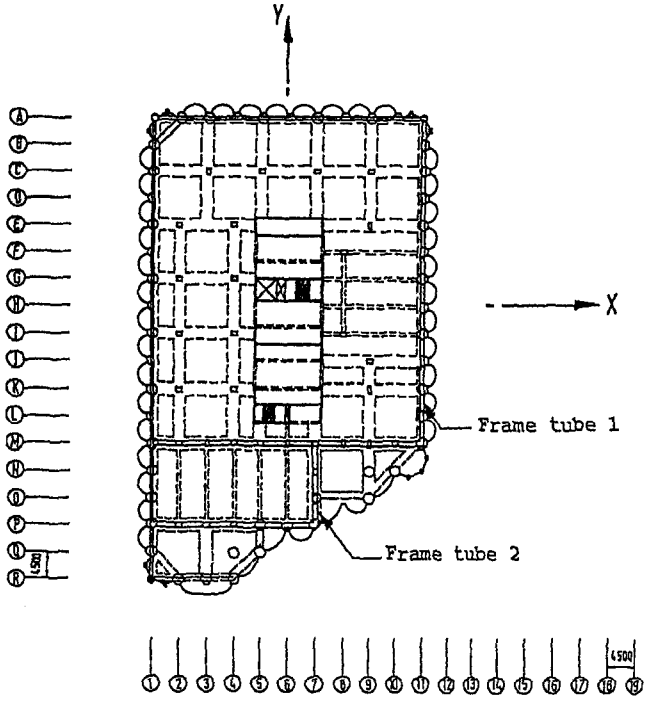

Fig. 6. Typical floor plan above 52nd storey.

rendered deeper by upturning the beam to the bottom of the window sill. Greater depth can be allowed for the spandrel beams between the windows and/or doors in consecutive floors without increasing floor to floor height. The shear and torsional rigidities can be further enhanced

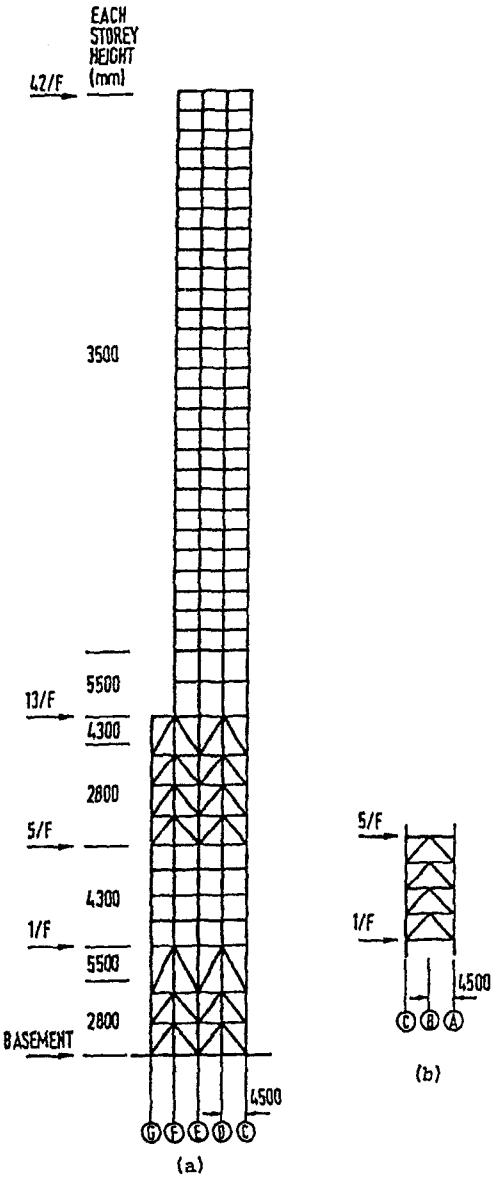

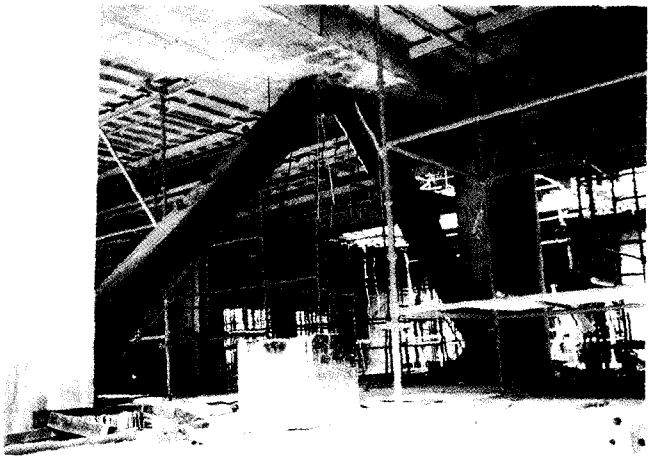

Fig. 7. Frame elevation showing K-bracings (a) along grid line 19, (b) along grid lines 11, 13 and 15, (c) K-braced frame.

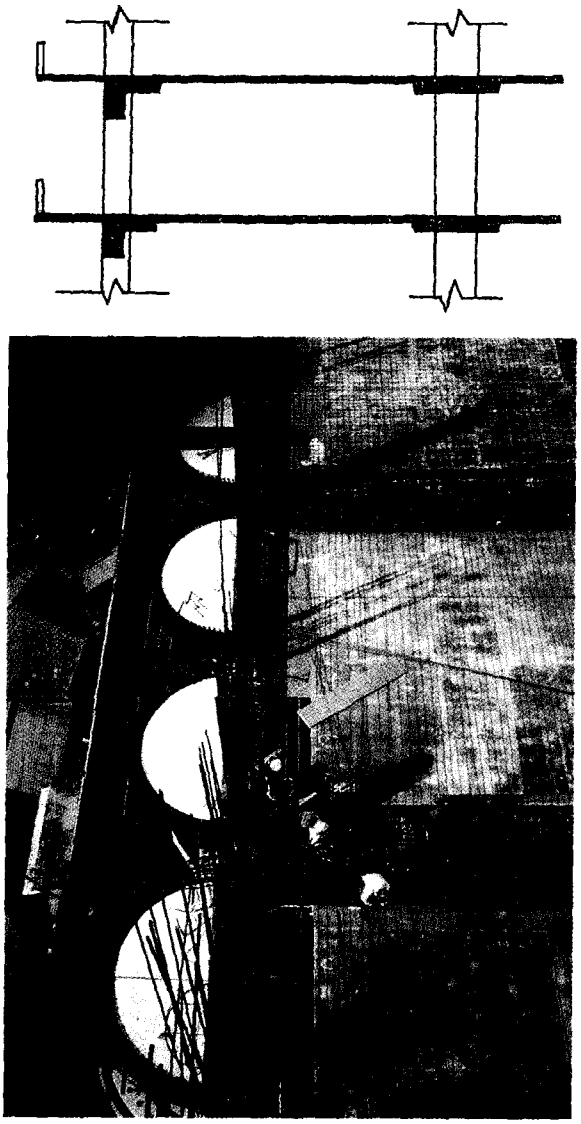

Fig. 8. Periphery frame tube and flat beam-slab system.

through the closer spacing of the periphery columns in the upper three quarters of the building.

Conventional flat slab is adopted for the ground floor and the basement car park with 9 m column spacing to facilitate car parking. A flat beam and slab system (Fig. 8) which is lighter is adopted for all other floors to carry vertical loads only. In the latter, the shear forces and bending moments in the column strip are resisted by the flat beam and the smaller shear forces and bending moment in the middle strip is resisted by the thin slab. This permits a lower storey height resulting in a substantial reduction in total building height and weight and thus allowing a leaner substructure system. Composite steel reinforced concrete columns are employed in the lower part of the building and ordinary reinforced concrete columns are used in the upper portion where the column loads are lighter. Loads from steel stanchions are transferred to reinforced concrete bored piles through shear studs. The use of composite steel reinforced concrete column for the lower portion of the building is necessary to reduce substantially the size of the columns and, more important, the steel stanchion is required if up-down construction method is adopted to dispense with the temporary excavation support system and to reduce the time of construction.

Tall buildings are usually supported by reinforced concrete rafts of 2.0 – 4.0 m thick under the tower but reduced to 1.5 – 2.0 m under the podium, if any. The raft usually rests on piles the type of which depends on the soil conditions at the site (Lee and Swaddiwudhipong, 1996). Due to the high column load and limited building area for tall buildings located in city centres, the piles are often spaced close together and in many cases, less than 3 pile diameter centre to centre. The pile interaction resulting from the close spacing has to be considered for the pile design by reducing the frictional capacity of the pile. The base of bored piles is sometimes grouted using high pressure stage grouting with tube-a-manchettes to increase bearing capacity and reduce settlement in the foundation system. The applied grouting pressure, up to 60 bars, is also a form of test loading the end bearing and frictional capacity of the pile. With base grouting, the increase in the cost of foundation is about 10% but the increase in ultimate bearing capacity is about 25-30% in this case. For deep excavation with the presence of deep soft clay layer at this site located in the vicinity of old buildings, diaphragm wall supported by the permanent basement slabs using top-down construction method is adopted for basement construction. The system provides a rigid excavation support system dispensing unnecessary cost for temporary works. In up-down approach, the construction of the substructure and superstructure may proceed concurrently saving the construction time by 10-20% in this case.

3. Structural Modelling

Core walls when subjected to lateral loads will deform in flexural mode, while frame tubes or rigid frames suffer shear deformation (Fig. 9). A tall building comprising frames and shear walls coupled together under transverse loading will deform as a shear- flexure cantilever and the equations of motion for the system can be obtained by superimposing the two components. Neglecting the effect of axial deformations, the governing equations for the vibration of the building can be expressed as (Balendra *et al.*, 1984).

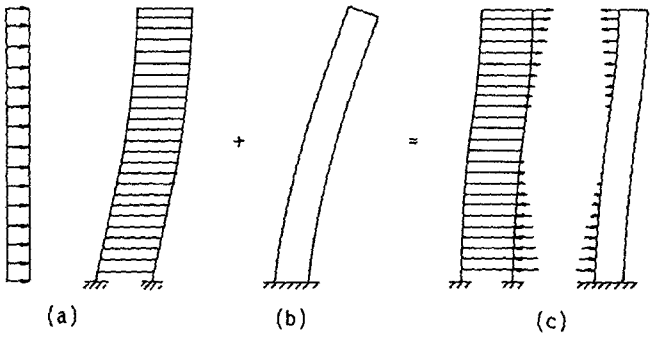

Fig. 9. Behaviour of frame shear wall structure under lateral load (a) shear mode, (b) flexural mode, (c) combined mode.

$$\begin{bmatrix}(EI_{yy}) & 0 & 0\\ 0 & (EI_{xx}) & 0\\ 0 & 0 & (EI_{ww})\end{bmatrix}\begin{Bmatrix}u^{iv}(z,t)\\ v^{iv}(z,t)\\ \theta^{iv}(z,t)\end{Bmatrix}$$

$$-\begin{bmatrix}(GA_{xx}) & 0 & 0\\ 0 & (GA_{yy}) & 0\\ 0 & 0 & (GJ_{ww})\end{bmatrix}\begin{Bmatrix}u''(z,t)\\ v''(z,t)\\ \theta''(z,t)\end{Bmatrix}$$

$$+\begin{bmatrix}m & 0 & -y_c\cdot m\\ 0 & m & x_c\cdot m\\ -y_c\cdot m & x_c\cdot m & (x_c^2+y_c^2+r^2)\cdot m\end{bmatrix}\begin{Bmatrix}\ddot{u}(z,t)\\ \ddot{v}(z,t)\\ \ddot{\theta}(z,t)\end{Bmatrix}=\begin{Bmatrix}f_u(z,t)\\ f_v(z,t)\\ f_\theta(z,t)\end{Bmatrix}$$

or in index notation as

$$EI_{ij}u_j^{iv}(z,t)-GA_{ij}u_j''(z,t)+m_{ij}\ddot{u}_j(z,t)$$
$$=q_i(z,t),i,j=1,2,3 \qquad (1)$$

where EI_{ij} the flexural (EI_{yy} and EI_{xx}), warping (EI_{ww}) stiffness matrix, and GA_{ij} the shear (GA_{xx} and GA_{yy}) torsional (GJ_{ww}) rigidity matrix, m_{ij} is the distributed mass matrix, u_j the displacement (u, v and θ) vector, f_i the force (f_u, f_v and f_θ) vector, x_c and y_c are coordinates of the mass centroid to the centre of resistance of each component and r is the radius of gyration of its mass centroid.

The flexural stiffness matrix is provided solely by cores and shear walls. Rigid jointed frames or frame tubes contribute predominantly to shear stiffness matrix. Both core walls and frames contribute to the torsional stiffness. The evaluation of EI_{ij} and GJ_{33} from core walls is a standard procedure and needs no further discussion. The determination of GA_{ij} for a frame tube is based on the assumption that the points of contra-flexure in both connecting beams and columns are at their mid length. The contribution from a panel of a storey shown in Fig. 10 to GA_{ij} can be shown to be

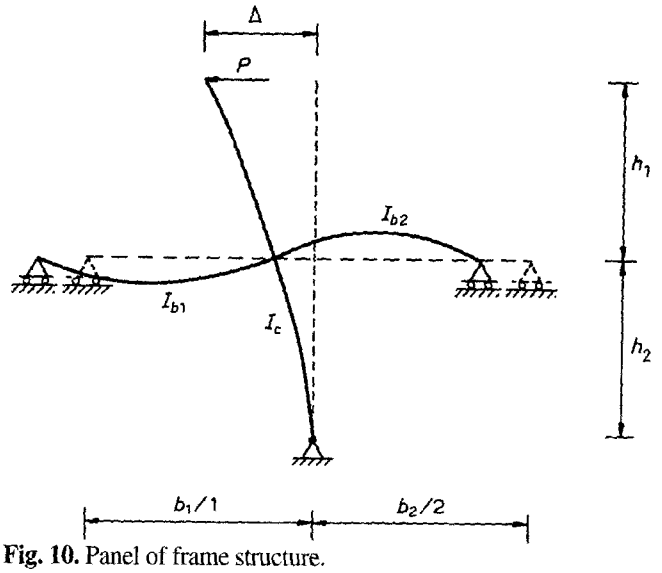

Fig. 10. Panel of frame structure.

$$GA_{ij}=\frac{6E}{\frac{2}{h_1+h_2}\left[\frac{h_1^3}{I_{c1}}+\frac{h_2^3}{I_{c2}}\right]+\frac{h_1+h_2}{\left[\frac{I_{b1}}{b_1}+\frac{I_{b2}}{b_2}\right]}} \qquad (2)$$

where E is the Young's modulus of elasticity, h_1 and h_2 are half storey height above and below that floor, b_1 and b_2 the length of beams on left and right, and I_{c1}, I_{c2}, I_{b1} and I_{b2} are the second moment of area of columns above and below the beams on the left and right respectively.

The torsional rigidity of the building can be substantially improved when the rigid jointed frames are arranged to form a frame tube or a bundle of frame tubes. For the latter case, as the building deforms as a unit, each frame tube share a common rate of angle twist, $d\theta/dz$. For tube α (Murray, 1984)

$$\frac{d\phi}{dz}=\frac{1}{2A_\alpha G}\left[\oint\frac{Q_\alpha}{t_\alpha}ds\right] \text{ or } \frac{1}{2A_\alpha}\left[\oint\frac{Q_\alpha}{G\frac{d\theta}{dz}}\frac{ds}{t_\alpha}\right]=1 \qquad (3)$$

where A_α and Q_α are the area enclosed by and shear flow provided by the frame tube α respectively and t_α is the thickness of the element ds on the perimeter of the tube.

The shear rigidity of side k forming the frame tube is expressed as

$$(GA_{ij})_k=Gt_kl_k \qquad (4)$$

where l_k is the length of frame k. The thickness t_k can be determined from Eq. (4), once $(GA_{ij})_k$ is evaluated from Eq. (2). Introducing $\varphi_\alpha=\frac{Q_\alpha}{G\frac{d\theta}{dz}}$, Eq. (3), in view of Eq. (4), for

a bundle of m frame tubes, can be expressed respectively as

$$1 = \frac{1}{2A_1}\left[\varphi_1\left(\sum\frac{l_k}{t_k}\right)_1 - \varphi_2\left(\sum\frac{l_{12}}{t_{12}}\right) - \cdots - \varphi_m\left(\sum\frac{l_{1m}}{t_{1m}}\right)\right]$$

$$1 = \frac{1}{2A_2}\left[-\varphi_1\left(\sum\frac{l_{12}}{t_{12}}\right) - \varphi_2\left(\sum\frac{l_k}{t_k}\right)_2 - \cdots - \varphi_m\left(\sum\frac{l_{2m}}{t_{2m}}\right)\right]$$

$$\vdots \qquad \vdots \qquad\qquad \vdots$$

$$1 = \frac{1}{2A_m}\left[-\varphi_1\left(\sum\frac{l_{1m}}{t_{1m}}\right) - \varphi_2\left(\sum\frac{l_{2m}}{t_{2m}}\right) - \cdots + \varphi_m\left(\sum\frac{l_k}{t_k}\right)_m\right] \quad (5)$$

where $l_{\alpha\beta}$ and $t_{\alpha\beta}$ are the length and thickness common to tubes α and β.

Solving Eqs. (5) for φ_1, φ_2, ... and φ_m, the torsional rigidity of a bundle of m tubes can be determined from

$$GJ_{ww} = 2\sum_{\alpha=1}^{m}(G\varphi_\alpha A_\alpha) \quad (6)$$

Any vertical axis may be chosen as the reference axis for the global system. However, to ensure that the stiffness matrices in the governing equations are numerically healthy, the axis in the vicinity of the resisting centre of the building is usually selected as the reference axis. All structural properties formulated based on the resisting centre of each component can be transferred to a common global reference axes through transformation matrices comprising both rotational and translational operations as described earlier in Balendra *et al.* (1984).

Assuming that the displacement vector to be a function of time and space independently, i.e.,

$$u_j(z,t) = \hat{u}_j(z)\cdot e^{i2\pi nt},\ j=1,2,3 \quad (7)$$

where n is the natural frequency in Hertz. For free vibration, Eq. (1) becomes

$$EI_{ij}\hat{u}_j^{iv}(z) - GA_{ij}\hat{u}_j''(z) - (2\pi n)^2 m_{ij}\hat{u}_j(z) = 0, i,j = 1,2,3 \quad (8)$$

The building is usually divided vertically into several uniform segments. For each segment, the EI, GA and distributed mass can be evaluated with respect to the same reference axis. The idealized geometric boundary conditions for a fixed support at the base are expressed as

$$\left.\begin{aligned}\hat{u}_j(0) &= 0\\ \hat{u}_j(0) &= 0\end{aligned}\right\},\ j=1,2,3 \quad (9)$$

and the mechanical boundary conditions at the top of the building of height H as

$$\left.\begin{aligned}GA_{ij}\hat{u}_j'(H) - EI_{ij}\hat{u}_j'''(H) &= 0\\ EI_{ij}\hat{u}_j''(H) &= 0\end{aligned}\right\},\ j=1,2,3 \quad (10)$$

Eq. (8) can be solved by Galerkin method of weighted residual. Let

$$\hat{u}_j = \delta_{sj}\alpha_{sr}\psi_{jr},\ j,s=1,2,3;\ r=1,2,...,p \quad (11)$$

where α_{sr} are the unknown parameters, ψ_{jr} the shape functions and δ_{sj} the well-known Kronecker delta function. Applying the Galerkin technique to Eq. (8) using the boundary conditions in Eqs. (9) and (10), integrating by parts and simplifying yield the following eigenvalue problem:

$$\int_0^h (EI_{ij}\psi_{js}''\psi_{kr}'' + GA_{ij}\psi_{js}'\psi_{kr}' - (2\pi n)^2 m_{ij}\psi_{js}\psi_{kr})\, dz\,\delta_{ik}\delta_{qj}\alpha_{qs} = 0$$

$$i,j,k,q = 1,2,3;\ r,s = 1,2,\cdots,p \quad (12)$$

from which the natural frequencies, n_q, are obtained and the corresponding eigenvectors, α_{qs}, give the various mode shapes.

4. Characteristics of Wind

The wind speed at elevation z can be written as

$$\hat{U}(z,t) = \bar{U}(z) + U(z,t) \quad (13)$$

where the mean wind speed $\bar{U}(z)$ is commonly the average wind velocity over one hour and $U(z,t)$ is the fluctuating component. Either the power or logarithmic laws are usually adopted to describe the variation of $\bar{U}(z)$ for different terrains.

Owing to the turbulence of the wind flow, the wind speeds vary randomly with time. An overall measure of the intensity of turbulence is given by the root mean square (RMS) value of the velocity fluctuations $\bar{U}(z)$ of the form

$$\sigma_u(z) = \left[\frac{1}{T_0}\int_0^{T_0} U^2(z,t)dt\right]^{1/2} \quad (14)$$

where T_0 is the averaging period which the fluctuating wind component is assumed to be stationary, normally taken as 1 hr. The non-dimensional turbulence intensity is expressed as

$$I(z) = \frac{\sigma_u(z)}{\bar{U}(z)} \quad (15)$$

A description of short term velocity fluctuations is provided by the power spectrum which indicates the power of kinetic energy per unit of time associated with eddies of different frequencies n. An expression of a power spectrum of wind is given by Simiu and Scanlan (1986) as

$$nS_u(z,n) = \frac{200fU^{*2}}{(1+50f)^{5/3}} \tag{16}$$

where $f = \frac{nz}{\overline{U}(z)}$ is the reduced frequency. The time-dependent drag force can be expressed as

$$\hat{f}_D(z,t) = \frac{1}{2}\rho C_D B[\overline{U}^2(z) + 2U(z,t)\overline{U}(z) + U^2(z,t)]$$

$$= \overline{f_D}(z) + f_D(z,t) + f_D'(z,t) \tag{17}$$

in which ρ is the air density; C_D is the drag coefficient, the values of which are given in Laneville *et al.* (1977) and Wooton and Scruton (1971); B is the width of the building; $\overline{f_D}(z,t)$ is the static mean wind pressure, $f_D(z,t)$ is the randomly fluctuating wind pressure and $f_D'(z,t)$ involving $U^2(z,t)$ is small and usually neglected. The characteristics of $f_D(z,t)$ can be established through its spectral density:

$$S_{f_D}(z,n) = \rho^2\overline{U}^2(z)B^2C_D^2S_u(z,n) \tag{18}$$

5. Structural Response to Wind Load

The wind flow around a building is three-dimensional. The along-wind response comprises the static mean and randomly fluctuating wind pressure. The latter is established through random vibration theory. The across-wind and torsional forces are highly correlated statistically and the former relates to both mean wind velocity and incident turbulence. The prediction of across-wind and torsional response of the building still relies heavily on experimental results. As the wind power attenuates rapidly with increasing frequency, only the contribution of the fundamental mode in each direction is considered. Introducing the damping effect, the governing equation can be expressed as:

$$m(z)\ddot{u}(z,t) + c(z)\dot{u}(z,t) + k(z)u(z,t) = f(z,t) \tag{19}$$

where k is the stiffness and c is the coefficient of viscous damping. Let

$$u(z,t) = \sum_i \phi_i(z)q_i(t) \tag{20}$$

in which the coefficients $q_i(t)$ are the generalized coordinates of the system and $\phi_i(z)$ are the vibration mode shapes. Eq. (19) becomes:

$$\ddot{q}_i(t) + 2\zeta_i(2\pi n_i)\dot{q}_i(t) + (2\pi n_i)^2 q_i(t) = \frac{F_t(t)}{M_t} \tag{21}$$

$$M_i = \int_0^H m(z)\phi_i^2(z)dz \tag{22}$$

$$F_i(t) = \int_0^H f(z,t)\phi_i(z)dz \tag{23}$$

ζ_i is the damping ratio and n_i the natural frequency of the building. The spectral density of the response $S_q(n)$ can be expressed using the spectral density of generalized force $S_F(n)$ as

$$S_{qi}(n) = |H_i(n)|^2 S_{F_i}(n) \tag{24}$$

where

$$|H_i(n)| = \frac{1}{4\pi^2 n_i^2 M_i \left\{\left[1-\left(\frac{n}{n_i}\right)^2\right]^2 + 4\zeta_i^2\left(\frac{n}{n_i}\right)^2\right\}^{1/2}} \tag{25}$$

The mean square value (variance) of the response can be written as:

$$\sigma_{q_i}^2 = \int_0^\infty S_{q_i}(n)dn = \int_0^\infty |H_i(n)|^2 S_{F_i}(n)dn \tag{26}$$

The integral in Eq. (26) is usually evaluated through the sum of the three components as illustrated in Fig. 11, i.e.,

$$\sigma_{q_i}^2 = \sigma_{q_i1}^2 + \sigma_{q_i2}^2 + \sigma_{q_i3}^2$$

$$= \int_0^{n_i-\Delta} S_{F_i}(n)|H_i(n)|^2 dn + \int_{n_i-\Delta}^{n_i+\Delta} S_{F_i}(n)|H_i(n)|^2 dn$$

$$+ \int_{n_i+\Delta}^{\infty} S_{F_i}(n)|H_i(n)|^2 dn$$

$$= \frac{1}{16\pi^4 n_i^4 (M_i)^2}\int_0^\infty S_{F_i}(n)dn + \frac{1}{16\pi^4 n_i^4 (M_i)^2}\frac{\pi n_i}{4\zeta_i} S_{F_i}(n_i)$$

$$= \sigma_{Bq_i}^2 + \sigma_{Dq_i}^2 \tag{27}$$

where $\sigma_{Bq_i}^2$ and $\sigma_{Dq_i}^2$ are, respectively, the background and resonant components of the response and $\sigma_{q_i3}^2$ is usually negligible. The corresponding mean square values of the two displacement components are

$$\sigma_{Bu}^2 = \sum_i \phi_i^2(z)\sigma_{B_{q_i}}^2 \tag{28}$$

$$\sigma_{Du}^2 = \sum_i \phi_i^2(z)\sigma_{D_{q_i}}^2 \tag{29}$$

5.1 Along-Wind Response

The most probable maximum displacement is obtained from (Davenport, 1964 and Engineering Science Data Unit, 1976)

$$u(z) = \bar{u}(z) + \{[g_B(z)\sigma_{Bu}(z)]^2 + [g_D(z)\sigma_{Du}(z)]^2\}^{1/2} \tag{30}$$

in which

$$g_B(z) = \{2\ln[\lambda_u(z)T_0/2\pi]\}^{1/2} \cong 3.5 \tag{31}$$

$$g_D(z) = \{2\ln[\lambda_u(z)T_0]\}^{1/2} + 0.577\{2\ln[\lambda_u(z)T_0]\}^{-1/2} \tag{32}$$

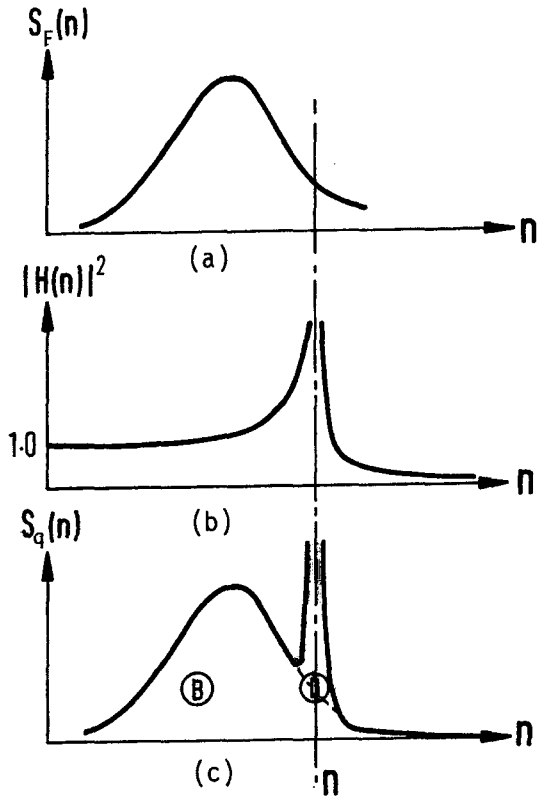

Fig. 11. Evaluation of variance of the response.

$$\lambda_u(z) = [\Omega_2(z)/\Omega_0(z)]^{1/2} \tag{33}$$

$$\Omega_i(z) = \int_0^\infty n^{(i)} S_u(z,n)dn \tag{34}$$

and T_0 is normally taken as 1 hour. For resonant component consisting mostly the response at the natural frequency n_u, the value of λ_u can be taken as n_u.

Similarly, the largest peak of the along-wing acceleration is approximated from

$$\ddot{u}(z) = g_{\ddot{u}}(z)\sigma_{\ddot{u}}(z) \tag{35}$$

where the root mean square value of acceleration is obtained from:

$$\sigma_{\ddot{u}}(z) = (2\pi n_u)^2 \sigma_{Du}(z) \tag{36}$$

The peak factor is

$$g_{\ddot{u}}(z) = \{2\ln[\lambda_{\ddot{u}}(z)T_0]\}^{1/2} + 0.577\{2\ln[\lambda_{\ddot{u}}(z)T_0]\}^{-1/2} \tag{37}$$

$$\lambda_{\ddot{u}}(z) = [\Omega_6(z)/\Omega_4(z)]^{1/2} \tag{38}$$

when substituting $z = H$, the maximum displacement u_{max} and the maximum acceleration $\ddot{u}_{max}$ in the along-wind direction can be obtained from Eqs. (30) and (35) respectively.

5.2 Across-Wind Response

The across-wind response is due principally to asymmetry of the wake flow. However, the lateral turbulent fluctuations in the incoming flow may also contribute to the across-wind forces. Standards Association of Australia, (1989) stipulates an expression for the acceleration at the top of a building as

$$\ddot{v}_{\max} = 1.5\frac{g_f \overline{q_H} B}{m_0}(0.76+0.24k)\left(\frac{\pi C_{fs}}{\zeta_v}\right)^{1/2} \tag{39}$$

where $g_f = \sqrt{[2\ln(3600n_v)]}$ is the peak factor in across-wind direction, $\overline{q_H}$ the hourly mean dynamic wind pressure at height H, in N/m^2, B the breadth of the structure normal to the wind in m, k a mode shape power exponent from representation of the fundamental mode shape of the form $\phi(z) = (z/H)^k$, C_{fs} the across-wind force spectrum coefficient generalized for a linear mode the values of which were given in chart form for buildings with square and rectangular sections (Standards Association of Australia, 1989), ζ_v the damping coefficient for across wind fundamental mode, m_0 the average mass per unit height of the structure in kg/m, and n_v the fundamental mode frequency in across-wind direction, in Hertz. The displacement at the top of the building can be obtained from

$$v_{max} = \frac{\ddot{v}_{max}}{(2\pi n_v)^2} \tag{40}$$

5.3 Torsional Response

The peak angular acceleration at the top of the building is

$$\ddot{\theta}(H) = \frac{2g_T T_{rms}(H)}{\rho_b BDHr_m^2} \tag{41}$$

where

$$T_{rms} = 0.00167\frac{1}{\sqrt{\zeta_\theta}}\rho L^4 H n_\theta^2 U_r^{2.68} \tag{42}$$

$$U_r = \frac{\overline{U(H)}}{n_\theta L} \tag{43}$$

$$L = \frac{\int |r| ds}{\sqrt{A}} \tag{44}$$

ρ_b is the mass density of the building, D is the depth of the building, r_m is the radius of gyration, g_T is the peak factor which can be taken as 3.8. ρ is the air density, n_θ and ζ_θ are the frequency and damping ratio in the fundamental torsional mode of vibration, $|r|$ is the distance between the elastic centre and the normal to an element "ds" on the

boundary of the building and A is the cross-sectional area of the building.

The peak angular displacement at the top of the building is evaluated from:

$$\theta(H) = \frac{1}{(2\pi n_\theta)^2}\ddot{\theta}(H) \tag{45}$$

The peak-torsional-induced horizontal accelerations and displacements in x- and y- directions at the top of the building are obtained respectively from:

$$\ddot{u}_{\theta max} = \ddot{\theta}(H)\cdot d_y,\ \ddot{v}_{\theta max} = \ddot{\theta}(H)\cdot d_x \tag{46}$$

$$u_{\theta max} = \theta(H)\cdot d_y,\ v_{\theta max} = \theta(H)\cdot d_x \tag{47}$$

where d_x and d_y are the distances from the elastic centre in x- and y- directions respectively.

5.4 Total Response

The peak combined effect of the along-wind, across-wind, and torsional loads can be obtained by summing up vectorially the individual peak effects of these loads and multiplying the result by a reduction factor of 0.8, which accounts for the fact that in general individual peaks do not occur simultaneously (Simiu and Scanlan, 1986).The peak resultant displacement and acceleration at the top of the building are

$$\Delta_{\max} = 0.8[(u_{\max}+u_{\theta\max})^2+(v_{\max}+v_{\theta\max})^2]^{1/2} \tag{48}$$

$$\ddot{\Delta}_{\max} = 0.8[(\ddot{u}_{\max}+\ddot{u}_{\theta\max})^2+(\ddot{v}_{\max}+\ddot{v}_{\theta\max})^2]^{1/2} \tag{49}$$

The values to be adopted shall be the larger of the combined effect or the individual peak.

Table 1. Structural response due to wind load in x-direction.

Structural Responses		As Adopted	Without Shear Walls	No Shear Walls and No Frame Tube Action
Peak Displacement (mm)	Along-Wind	131.1	189.2	189.2
	Across-Wind	83.3	95.9	95.9
	Due to Twist	11.9	26.6	64.4
	Total	137.5	198.6	240.0
	Most Probable	137.5	198.6	240.0
Peak Acceleration (milli-g)	Along-Wind	3.79	4.54	4.54
	Across-Wind	10.51	11.17	11.17
	Due to Twist	4.23	5.19	6.50
	Total	13.44	15.23	16.66
	Most Probable	13.44	15.23	16.66

5.5 Effect of Structural Eccentricity

The core wall of the 70-storey building described earlier is placed eccentrically due mainly to architectural requirements. The adverse effect of this eccentricity is reduced greatly through the introduction of a series of shear walls strategically located in the lower floors and the introduction of intermediate periphery columns in the frame tubes above the thirteenth floor. To demonstrate the effectiveness of these remedial measures, the responses under the same wind load environment of the following three

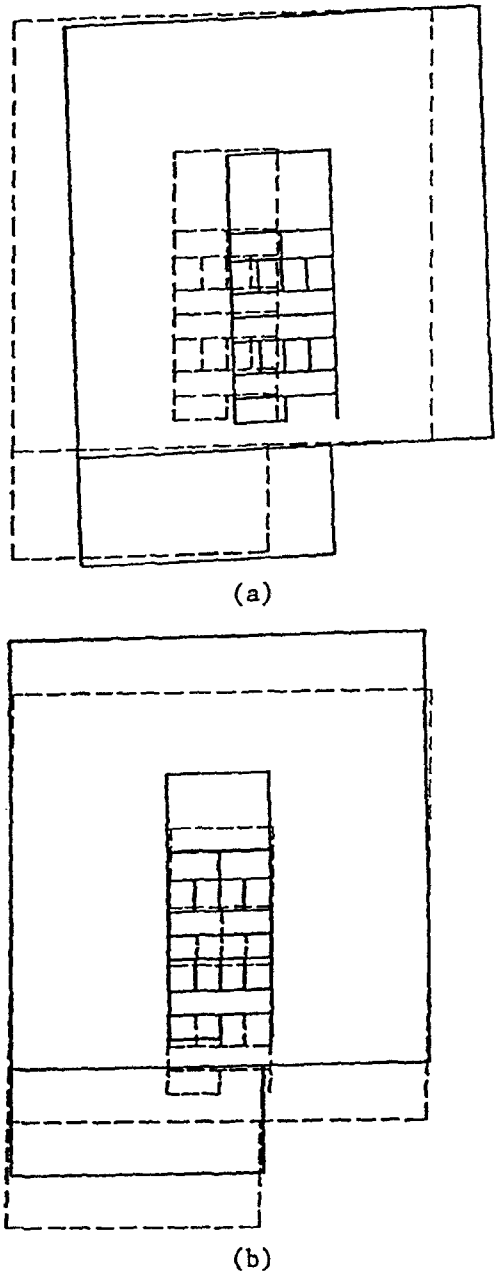

Fig. 12. Structural plans showing deflections at top of building under lateral loads in (a) x-direction and (b) y-direction.

structural systems are carried out. They are i) the system as adopted for construction, ii) the adopted system but without the presence of shear walls in the lower floors and iii) as in ii) but with no contribution from the tube actions. The results based on $\zeta_v = \zeta_\theta = 0.02$ are tabulated in Table 1. Actions resulting from the frame tubes configuration in the upper portion of the building reduce greatly the peak displacement due to twisting from 64 mm to 27 mm. The value decreases further to about 12 mm with the presence of heavy walls at the lower level. These shear walls also reduce substantially the along-wind peak displacement from 189 mm to 131 mm. The effect on the cross-wind peak displacement as well as peak acceleration at the top of the building is less pronounced. The peak displacement of 137.5 mm and the maximum acceleration of 13.44 milli-g of the building as constructed are within the acceptable ranges of values in common practice.

6. Concluding Remarks

The adopted structural system should provide efficient and cost effective resistance to lateral loads which can be achieved through (i) torsionally rigid closed frame tube comprising deep spandrel beams and flat columns at the periphery and/or bundle of frame tubes and (ii) proper distribution of flexural and shear rigidities of the building such that under lateral load, it will deflect mainly in the direction of the applied force without inducing substantial response in the transverse direction and/or twist as shown in Fig. 12 for the building discussed. Design of buildings, excepting the frame tube members and the shear walls, specially in mild wind environment and low seismic zone is usually proportioned initially on gravity loads and checked against lateral actions using established computer programmes with increased allowable stresses or reduced load factor for lateral loading. In the latter case, additional reinforcement and/or increase in member sizes may be required. The structural vibration due to wind load must satisfy requirements for comfort criteria and human perception to horizontal acceleration.

References

Balendra T, Swaddiwudhipong S, Quek ST, Lee SL (1984) Free vibration of asymmetric shear wall-frame buildings, Earthquake Eng. and Struct. Dyn., 12: 629-650.

Davenport AG (1964) Note on the distribution of the largest value of a random function with application to gust loading, Proc. Instn. Civil Engrs: 187-196.

Engineering Science Data Unit (1976) The Response of Flexible Structures to Atmospheric Turbulence, ESDU Item No. 76001, London.

Laneville A, Gartshore IS, Parkinson GV (1977) An Explanation of Some Effects of Turbulence on Bluff Bodies. Proc. Fourth Int. Conf. On Wind Effects on Buildings and Structures, Cambridge, UK.

Lee SL, Yong KY, Swaddiwudhipong S, Sitichaikasem S, Ratanaprichavej R (1992) Structural Design and Construction of 70-storey Concrete Building. Special Lecture, Proc. JCI Annual Convention Fukuoka, Japan Concrete Institute: 1-41.

Lee SL, Swaddiwudhipong S (1996) Up-Down Construction of Tall Buildings in City Centre. Proc. Int. Conf. on Urban Engineering in Asian Cities in the 21st Century, Bangkok, Thailand, 1: 22-45.

Murray NW (1984) Introduction to the Theory of Thin-walled Structures, Clarendon Press, Oxford.

Simiu E, Scanlan RH (1986) Wind Effects on Structures, 2nd Edition, John Wiley & Sons, New York.

Standards Association of Australia (1989) Minimum Design Loads on Structures (SAA Loading Code), Part 2: Wind Loads, Sydney, Australia.

Wooton LR, Scruton C (1971) Aerodynamic Stability, The Modern Design of Wind-sensitive Structures, Construction Industry Research and Information Association, London, UK: 65-81.